Recent results for hadron interactions in the HAL QCD method

Sinya Aoki

Center for Gravitational Physics,

Yukawa Institute for Theoretical Physics, Kyoto University

for

HAL QCD collaboration

BNL-HET & RBRC Joint workshop "DWQCD@25"

13-18 December 2021, Virtual Event

I. Introduction

Hadron interactions in lattice QCD

Finite volume method

spectra of two hadrons
in finite box

scattering phase shift

Luescher's finite volume formula

HAL QCD method

NBS wave functions

Potential
(Interaction kernel)

scattering
phase shift

Schrodinger equation

Today's topics

I. Introduction

II. Heavy dibaryons

III. Resonances in the HAL QCD method

IV. HAL QCD potentials in the moving systems

V. Summary and discussions

II. Heavy dibaryons

Y. Lyu, H. Tong, T. Sugiura, S. Aoki, T. Doi, T. Hatsuda, J. Meng, T. Miyamoto,
“Dibaryon with highest charm number near unitarity from lattice QCD”,
Phys. Rev. Lett. 127 (2021) 072003 (arXiv:2102.0081).

Baryon (B=1)

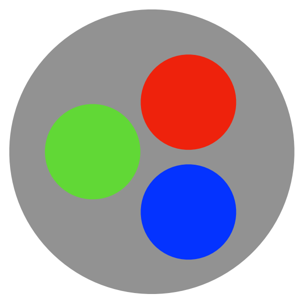

Proton, Neutron,
Lambda, Omega,…

Dibaryon (B=2)

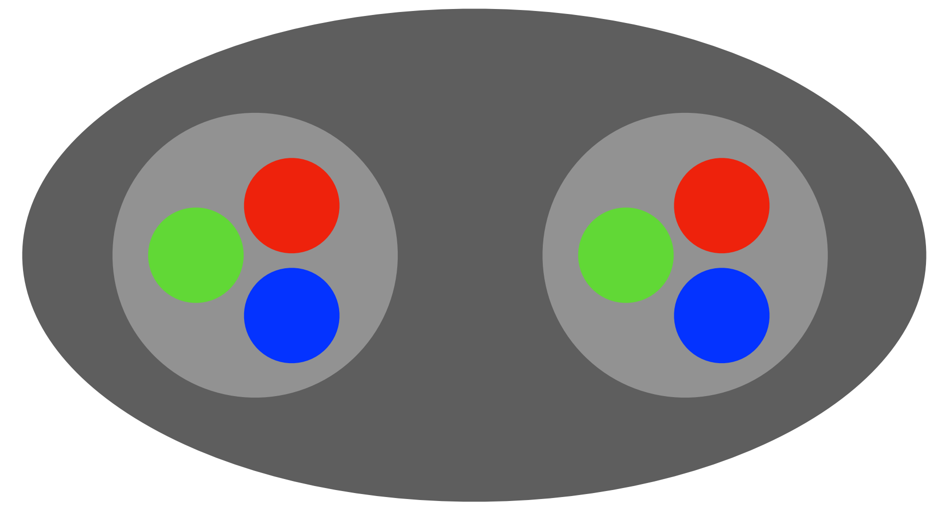

Deuteron
observed in 1930s
+ d*(2380) resonance

Dibaryon = two baryon bound state or resonance

Previous results

H dibaryon

T. Inoue et al. (HAL QCD Coll.), PRL106(2011)162002 — flavor SU(3) limit

K. Sasaki et al. (HAL QCD Coll.), NPA106(2020)121737 — physical point, $\Lambda\Lambda, N\Xi$

$\Delta\Delta$ dibaryons

S. Gongyo et al. (HAL QCD Coll.), PLB811(2020)135935 — flavor SU(3) limit, $d^*(2380)$

$N\Omega$ dibaryons

F. Etminan et al. (HAL QCD Coll.), NPA928(2014)89 — $m_\pi \simeq$ 875 MeV

T. Iritani et al. (HAL QCD Coll.), PLB792(2019)284 — physical point

$\Omega\Omega$ dibaryons

M. Yamada et al. (HAL QCD Coll.), PTEP 7(2015)187 — $m_\pi \simeq$ 700 MeV

S. Gongyo et al. (HAL QCD Coll.), PRL 120(2018)212001 — physical point

$\Omega_{ccc}\Omega_{ccc}$ dibaryons

Y. Lyu, et al., Pays. Rev. Lett. 127 (2021) 072003 (arXiv:2102.0081)

$\Omega(ccc)$: triply charmed baryon, stable against strong decay, mass/EM form factor

$\Omega(ccc)\Omega(ccc)$: S-wave& zero total spin, then no Pauli exclusion

↓

attractions ?

↓

bound state ?

HAL QCD method

R-correlator

$$R(\boldsymbol{r}, t>0) = \langle 0|\Omega_{ccc}(\boldsymbol{r}, t)\Omega_{ccc}(\boldsymbol{0}, t)\overline{\mathcal{J}}(0)|0\rangle / e^{-2m_{\Omega_{ccc}}t}$$
$$= \sum_n A_n \psi_n(\boldsymbol{r}) e^{-(\Delta W_n)t} + O(e^{-(\Delta E^*)t}),$$

non-local potential

$$\left(\frac{1}{4m_{\Omega_{ccc}}}\frac{\partial^2}{\partial t^2} - \frac{\partial}{\partial t} - H_0\right) R(\boldsymbol{r}, t) = \int d\boldsymbol{r}' U(\boldsymbol{r}, \boldsymbol{r}') R(\boldsymbol{r}', t),$$

derivarive expansion

$$U(\mathbf{r}, \mathbf{r}') = V(\mathbf{r})\delta^{(3)}(\mathbf{r} - \mathbf{r}') + \cdots$$

local potential

$$V(r) = R^{-1}(\boldsymbol{r}, t)\left(\frac{1}{4m_{\Omega_{ccc}}}\frac{\partial^2}{\partial t^2} - \frac{\partial}{\partial t} - H_0\right) R(\boldsymbol{r}, t).$$

at reasonably large t

Lattice setup

2+1 flavor gauge configuration on 96^4 lattice

with Iwasaki gauge + NP $O(a)$ improved clover quark

$a \simeq 0.0846$ fm, $m_\pi \simeq 146$ MeV, $m_K \simeq 525$ MeV (near physical point)

$La \simeq 8.1$ fm

(quenched) charm quark mass

	$(m_{\eta_c} + 3m_{J/\Psi})/4$ [MeV]	$m_{\Omega_{ccc}}$ [MeV]
set 1	3096.6(0.3)	4837.3(0.7)
set 2	3051.4(0.3)	4770.2(0.7)
Interpolation	3068.5(0.3)	4795.6(0.7)
Exp.	3068.5(0.1)	-

potential → scattering phase shift

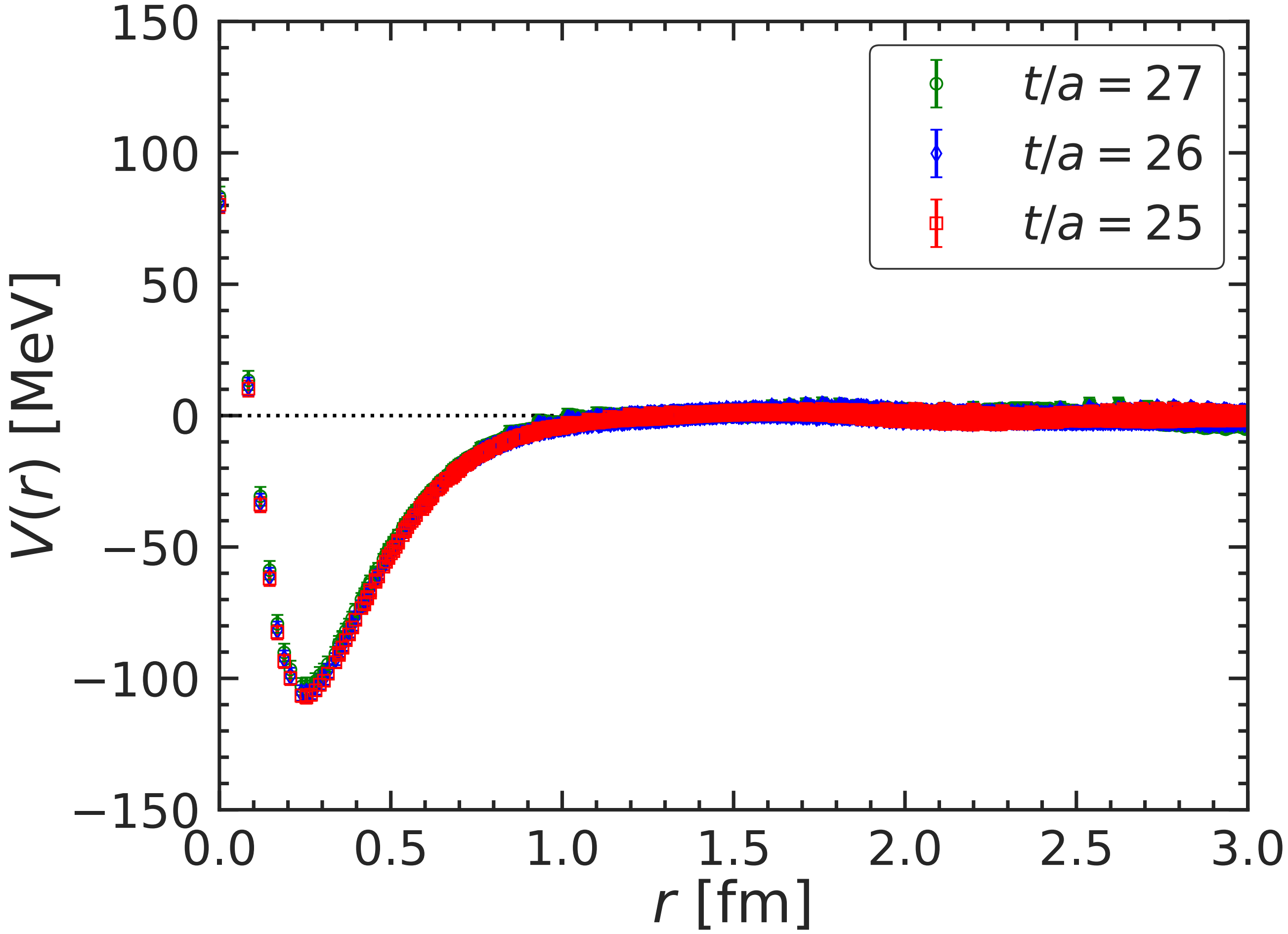

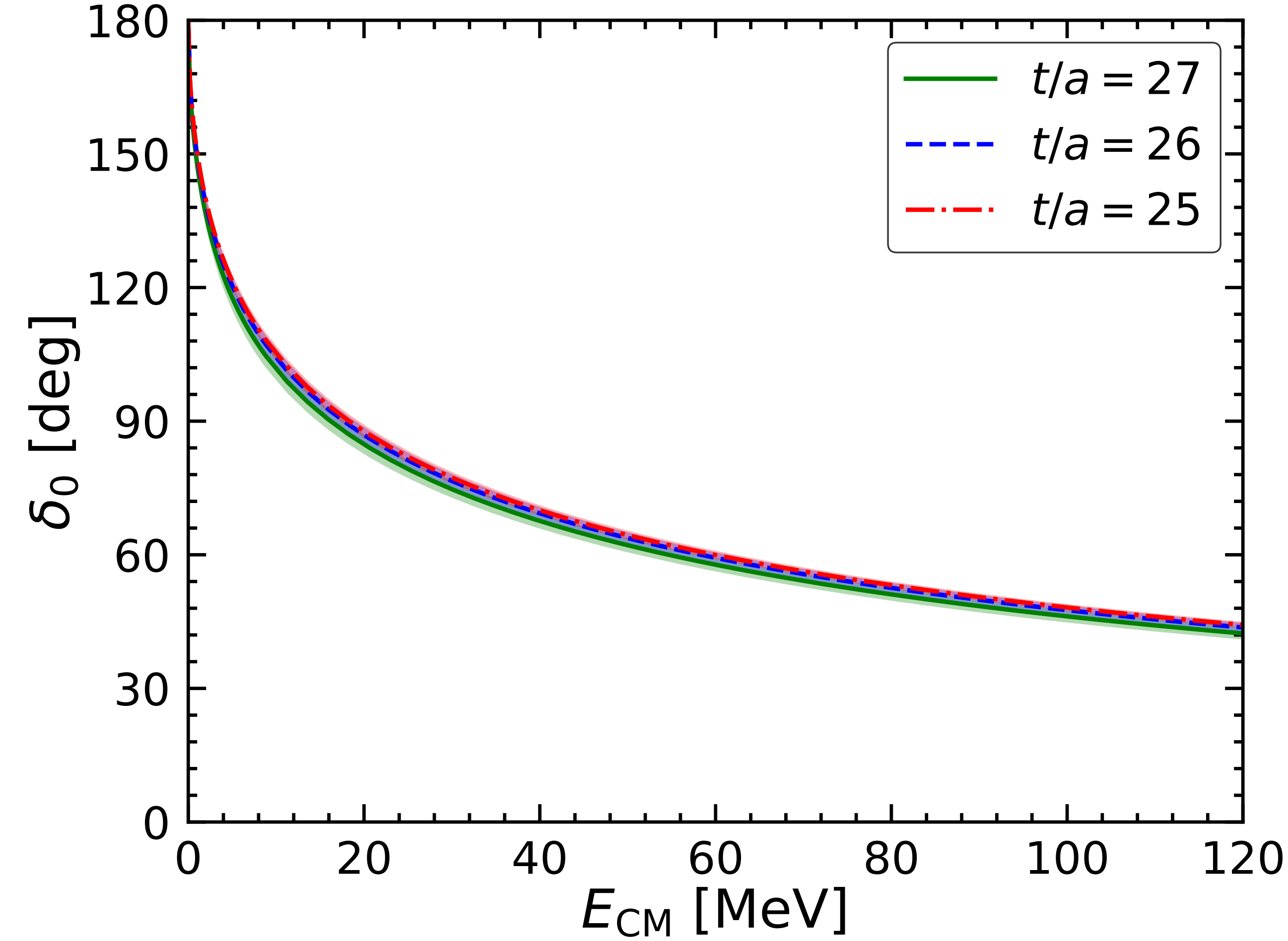

one bound state

$$B = 5.68(0.77)(^{+0.46}_{-1.02})\ \mathrm{MeV},$$ BE

$$\sqrt{\langle r^2 \rangle} = 1.13(0.06)(^{+0.08}_{-0.03})\ \mathrm{fm}.$$ size

Effective Range Expansion (ERE)

$$k \cot \delta_0(k) = -\frac{1}{a_0} + \frac{1}{2} r_{\mathrm{eff}} k^2 + O(k^4)$$

scattering length

$$a_0 = 1.57(0.08)(^{+0.12}_{-0.04})\ \mathrm{fm},$$

$$r_{\mathrm{eff}} = 0.57(0.02)(^{+0.01}_{-0.00})\ \mathrm{fm}.$$

effective range

$$B = \frac{(1 - \sqrt{1 - 2r_{\mathrm{eff}}/a_0})^2}{m_{\Omega_{ccc}} r_{\mathrm{eff}}^2} \simeq 5.7\ \mathrm{MeV}$$

$$\sqrt{\langle r^2 \rangle} = \frac{a_0}{\sqrt{2}} \simeq 1.1\mathrm{fm}$$

← loosely bound state

Coulomb repulsion

charge distribution inside Ω_{ccc}

$$\rho(r) = \frac{12\sqrt{6}}{\pi r_d^3} \exp\left[-\frac{2\sqrt{6}r}{r_d}\right]$$

charge radius of Ω_{ccc} $\quad r_d = 0.410(6)$ fm

K. U. Can, et al., Phys. Rev. D92 (2015) 114515.

Coulomb potential between two Ω_{ccc} 's

$$V^{\text{Coulomb}}(r) = \alpha_e \iint d^3r_1 d^3r_2 \frac{\rho(r_1)\rho(|\vec{r}_2 - \vec{r}|)}{|\vec{r}_1 - \vec{r}_2|}$$

$1/a_0^C$ vs. $\alpha_e/\alpha_e^{\text{phys.}}$

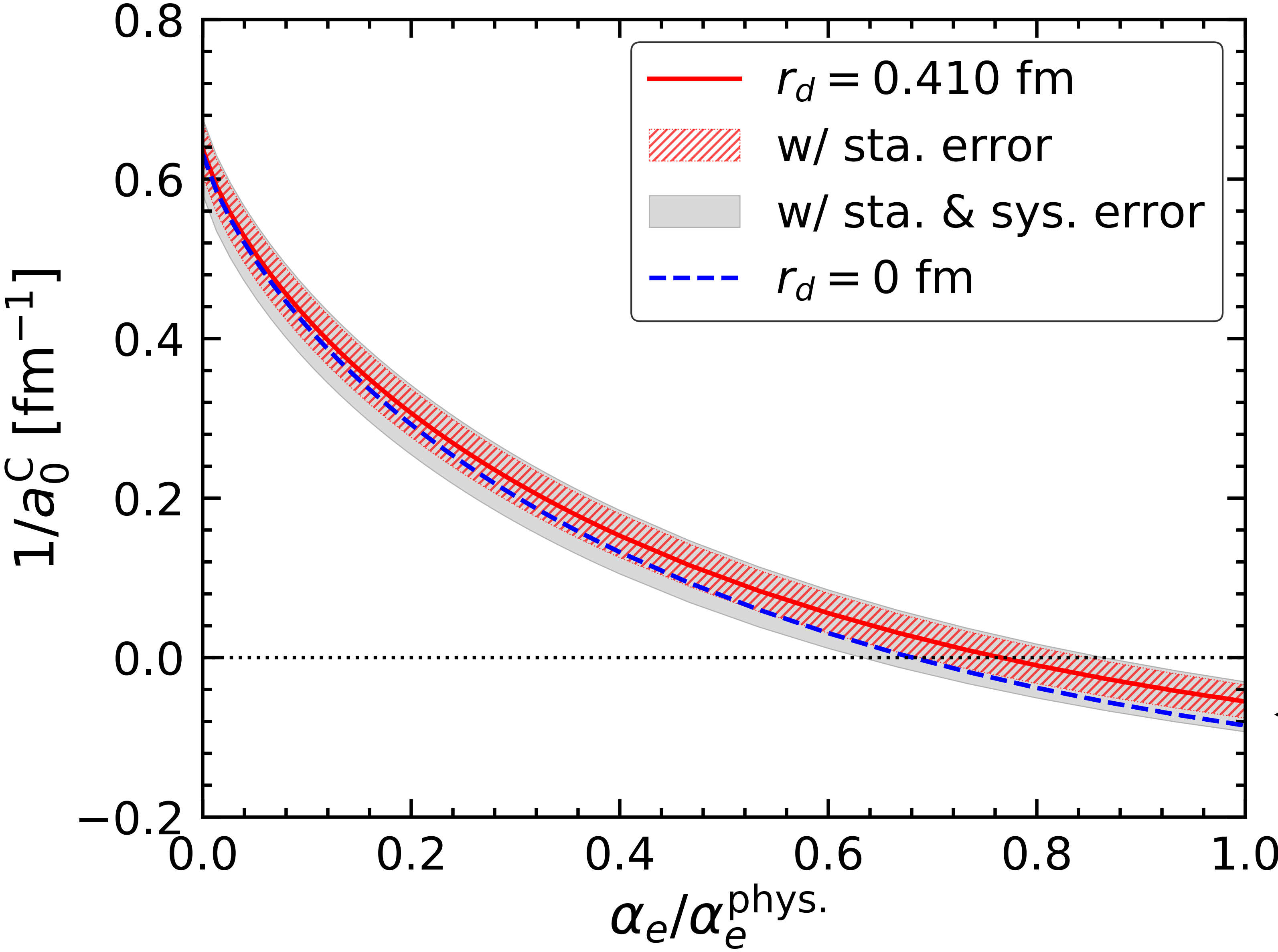

physical value

unbound

$$a_0^{\mathrm{C}} = -19(7)(^{+7}_{-6})\ \mathrm{fm},$$

unitary region

$$r_{\mathrm{eff}}^{\mathrm{C}} = 0.45(0.01)(^{+0.01}_{-0.00})\ \mathrm{fm}.$$

$r_{\mathrm{eff}}^C/a_0^C = -0.024(0.010)(^{+001}_{-0.00})$ fm

Comparison with other dibaryons

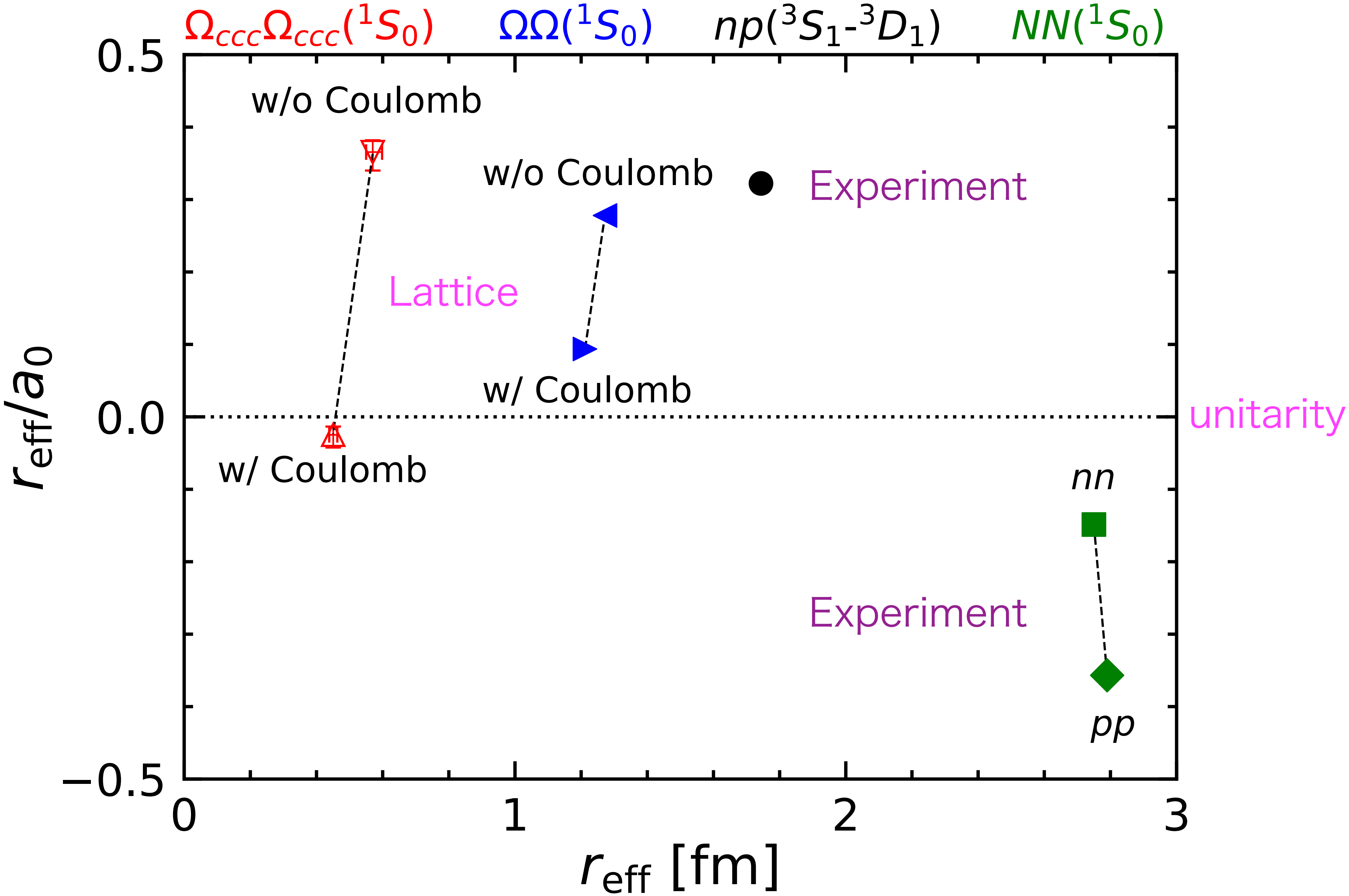

All “dibaryons” appear near unitarity. Why ?

$\Omega_{ccc}\Omega_{ccc}(^1S_0)$ dibaryon is closest to unitarity among these.

III. Resonance in the HAL QCD method

Y. Akahoshi, S. Aoki, T. Doi,

"Emergence of ρ resonance from the HAL QCD potential in lattice QCD",

Phys. Rev. D104 (2021) 054510 (arXiv:2106.08175).

ρ resonance

ρ meson is a resonance of $\pi\pi$ scattering

Can we reproduce ρ resonance form $I=1$ $\pi\pi$ HAL QCD potential ?

Obstructions/Difficulties

“box” diagram for $I=1$ $\pi\pi$ system

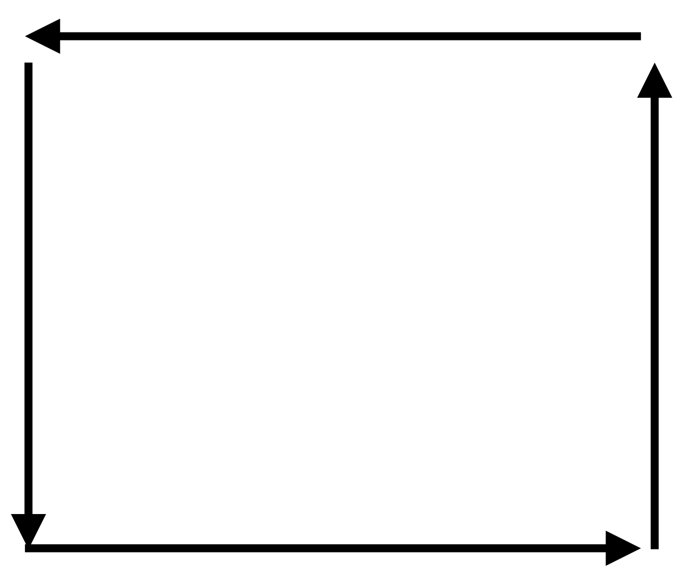

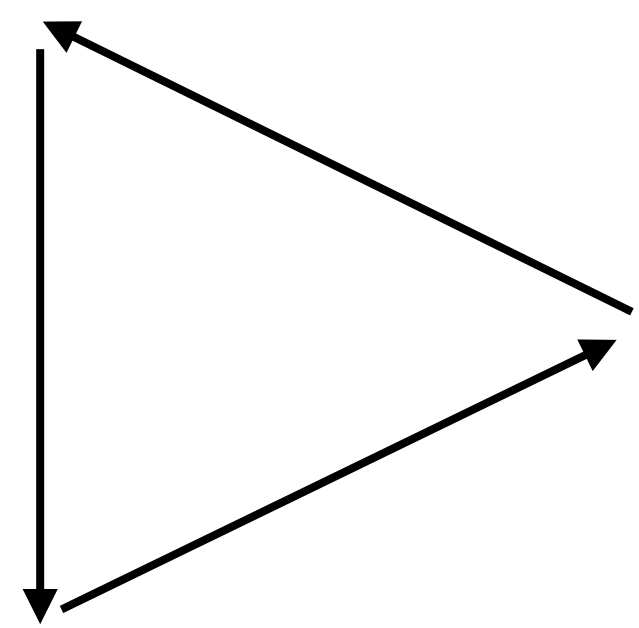

large numerical cost/noises

Our strategy

3 techniques for all-to-all propagators are combined.

- one-end trick — C. McNeill, C. Michael, PRD73 (2006) 074506.
- sequential propagator — G. Martinelli, C.T. Sachrajda, NPB316 (1989) 355.
- covariant approximation averaging (CAA) — E. Shintani, et al, PRD91 (2015) 114511.

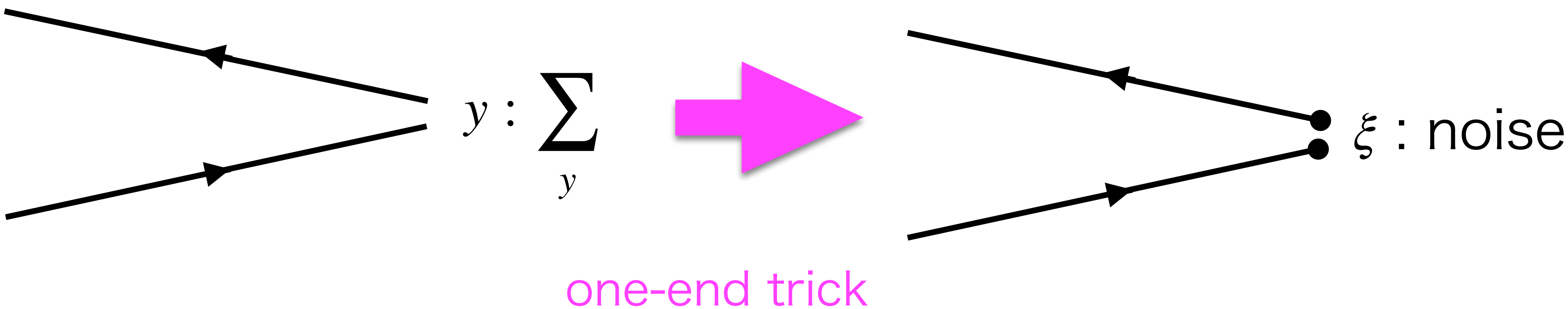

two (ρ and $\pi\pi$) sources → N^{2}LO analysis

smeared sink operators → remove short distance singularity expected by OPE

Diagrams

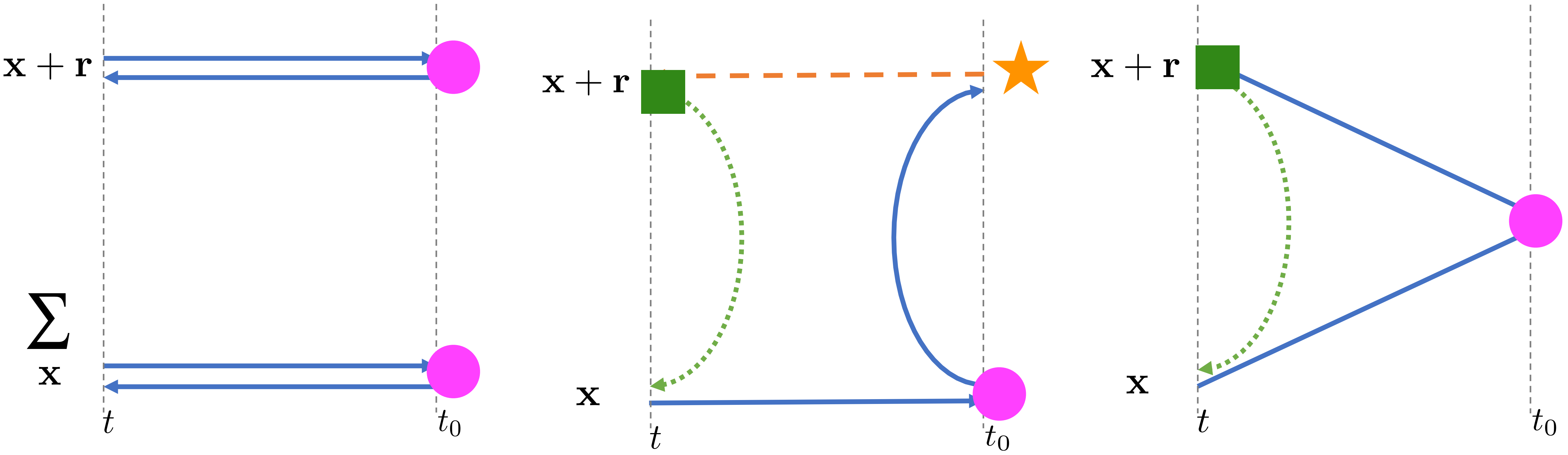

one-end trick summation over space

sequential source summation over space

CAA fixed point in space

Lattice setup

2+1 flavor gauge configuration on $32^3 \times 64$ lattice

with Iwasaki gauge + NP $O(a)$ improved clover quark

$a \simeq 0.0907$ fm, $m_\pi \simeq 411$ MeV, $m_\rho \simeq 892$ MeV (PACS-CS configurations)

$La \simeq 2.9$ fm

statistics

Source type	Scheme	$N_{\rm conf}$ (#. of time slice ave.)	Stat. error
$\pi\pi$-type	equal-time, smeared-sink	100 (64)	jackknife with bin–size 5
ρ-type	equal-time, smeared-sink	200 (64)	jackknife with bin–size 10

Results

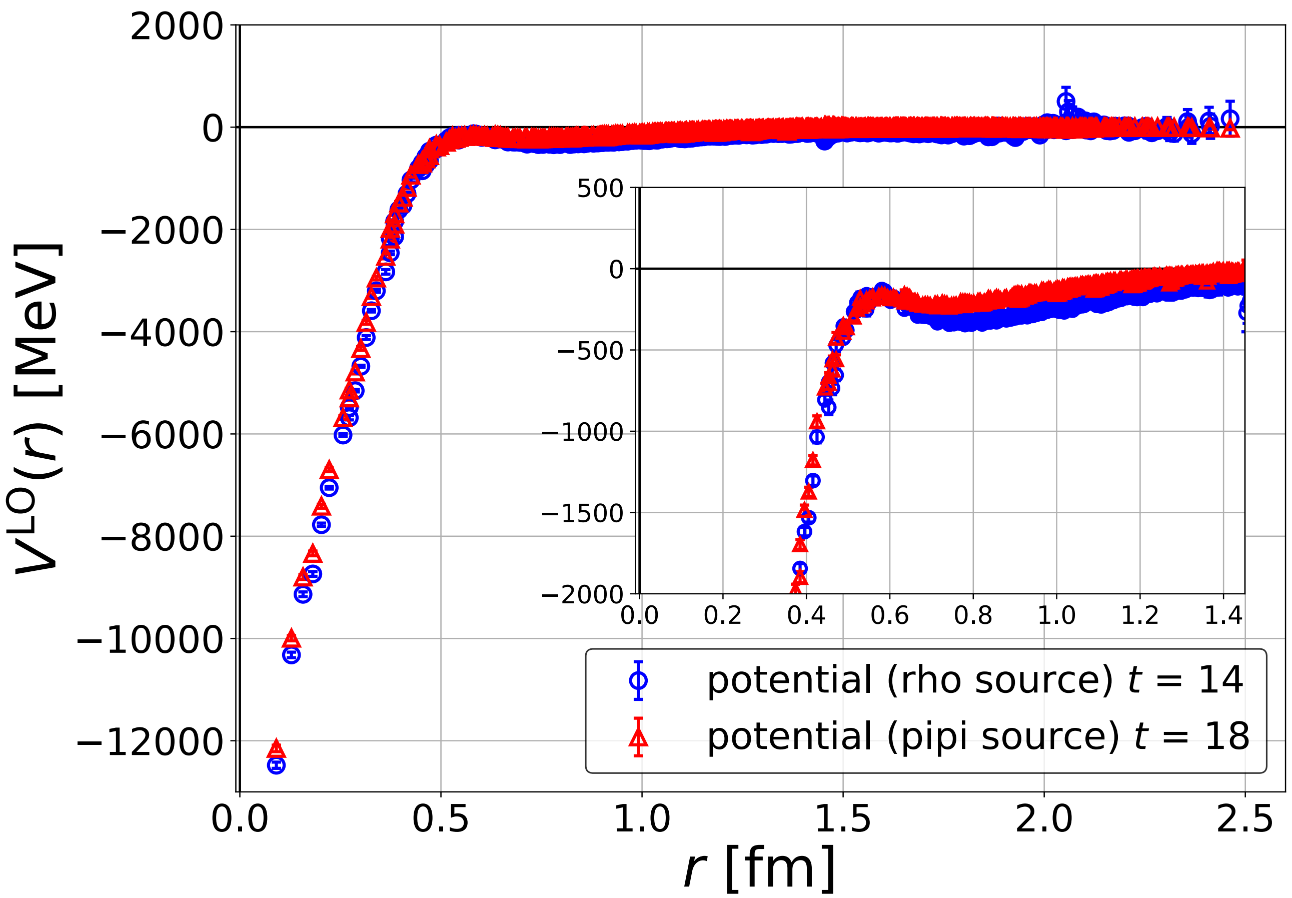

Leading order potentials
from ρ and $\pi\pi$ sources

apply a technique of higher
partial wave reduction

T. Miyamoto, et al, PRD101 (2020) 074514.

+ L=1 centrifugal term

$$V_C(r) = \frac{1}{2\mu}\frac{L(L+1)}{r^2}$$

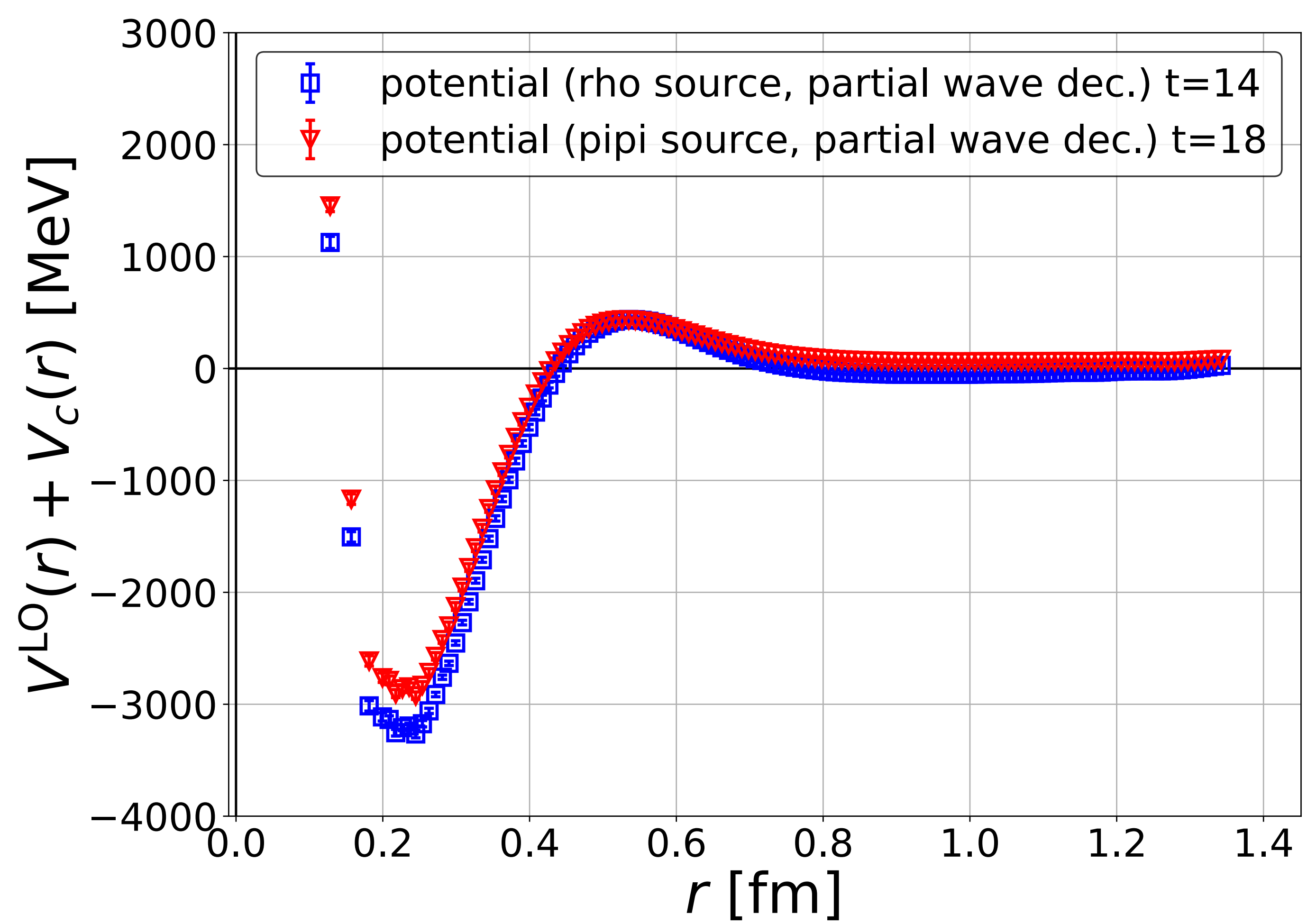

phase shift

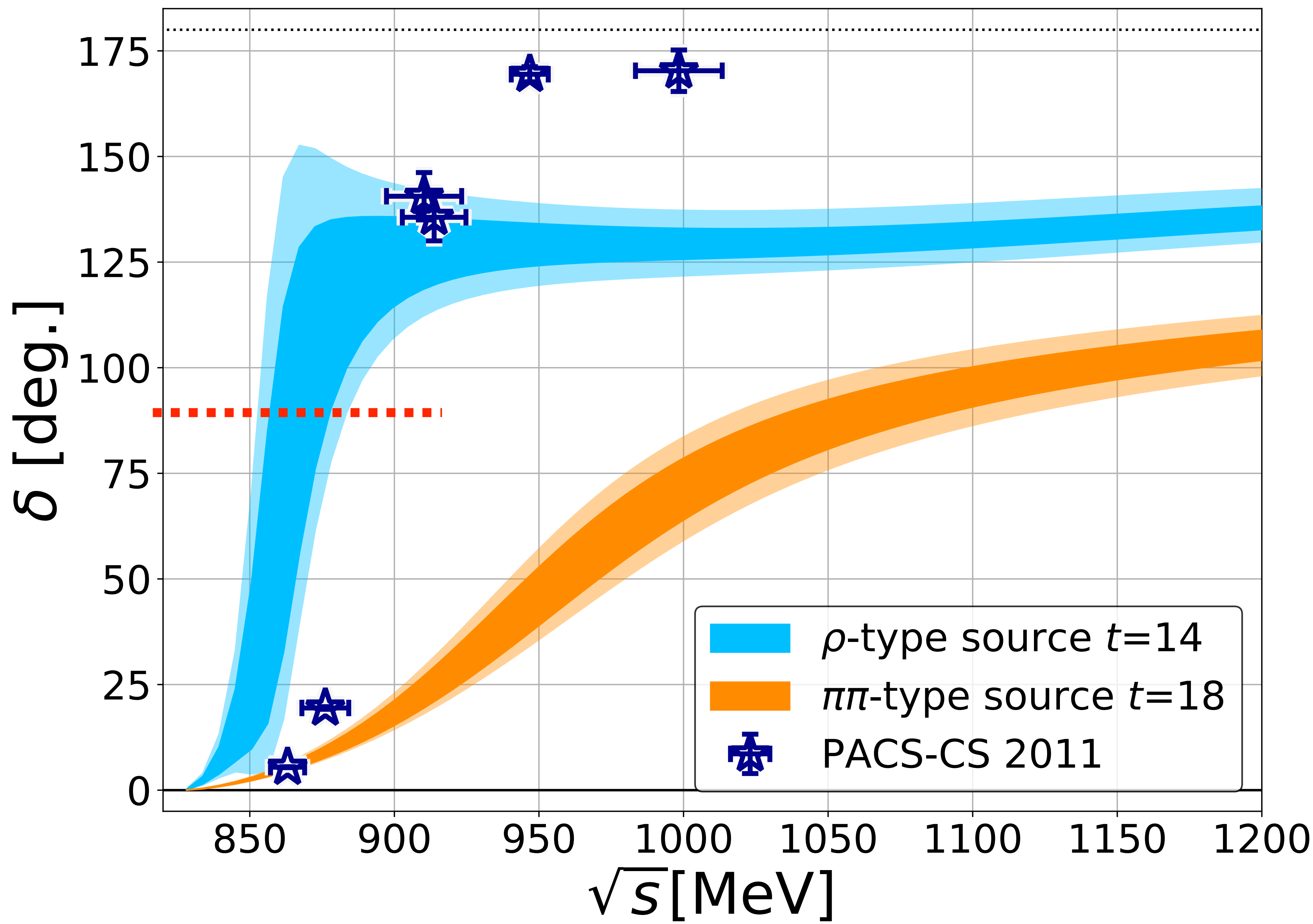

resonant behaviors are seen.

results from two sources differ. → N²LO analysis is mandatory.

they disagree with the FV spectra.

N²LO potential

$$U^{\mathrm{N^2LO}}(\mathbf{r},\mathbf{r}') = \left(V_0^{\mathrm{N^2LO}}(r) + V_2^{\mathrm{N^2LO}}(r)\,\nabla^2 \right) \delta(\mathbf{r}-\mathbf{r}')$$

$V_0^{\mathrm{N^2LO}}(r)$

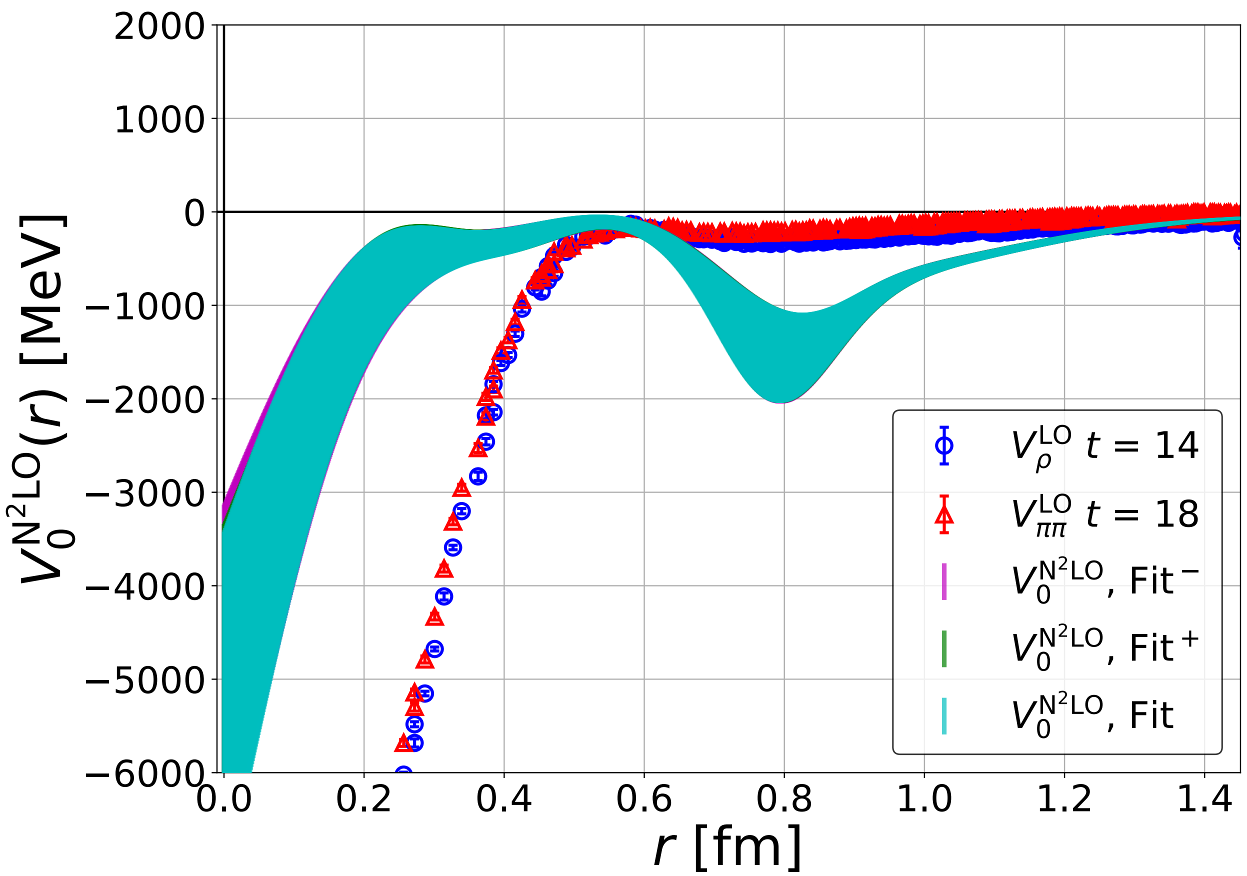

$V_2^{\mathrm{N^2LO}}(r)$

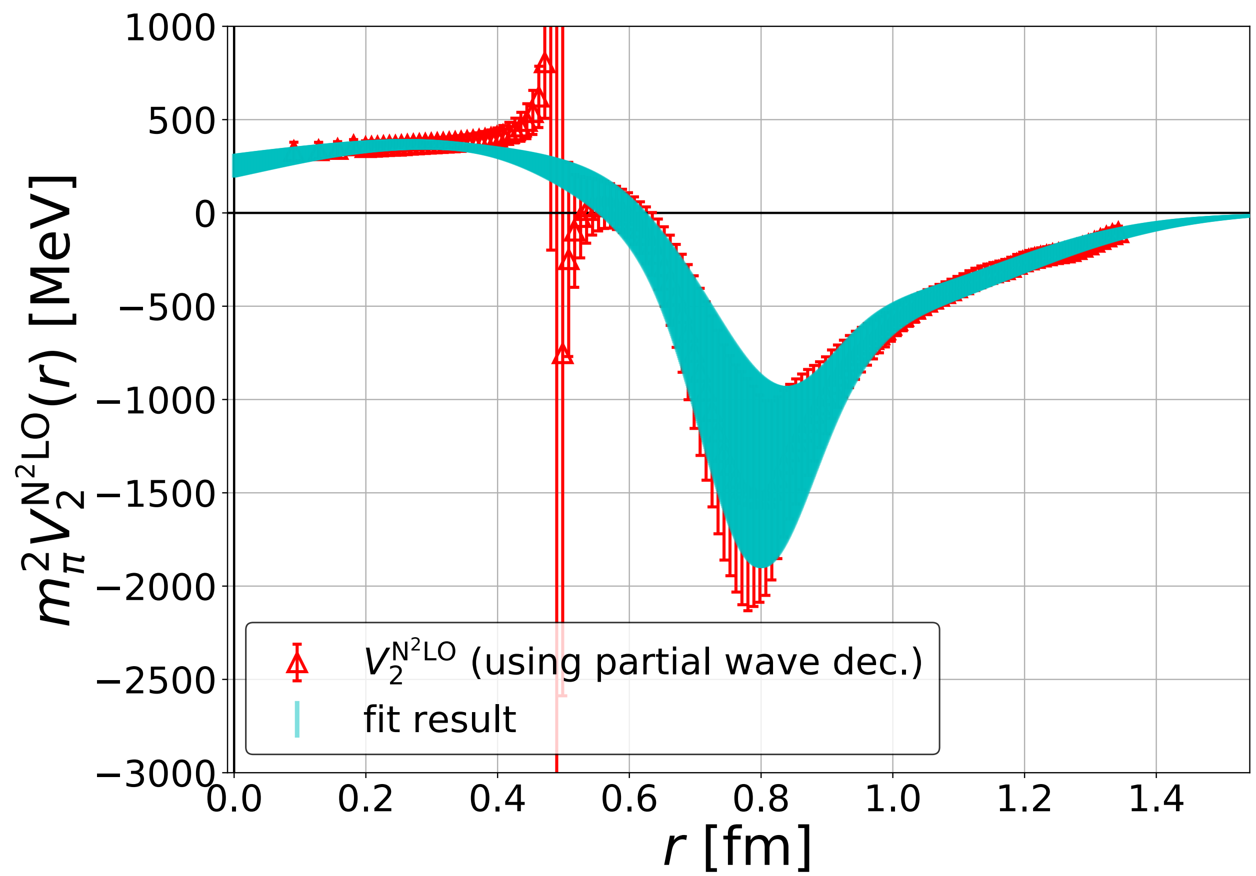

$V_0^{\mathrm{N^2LO}}(r)$ is obtained.

$V_2^{\mathrm{N^2LO}}(r)$ with large noises is fitted first.

cf. a singularity could be included.

S. Aoki, K. Yazaki, arXiv:2109.07665(hep-lat).

N^{2}LO phase shift

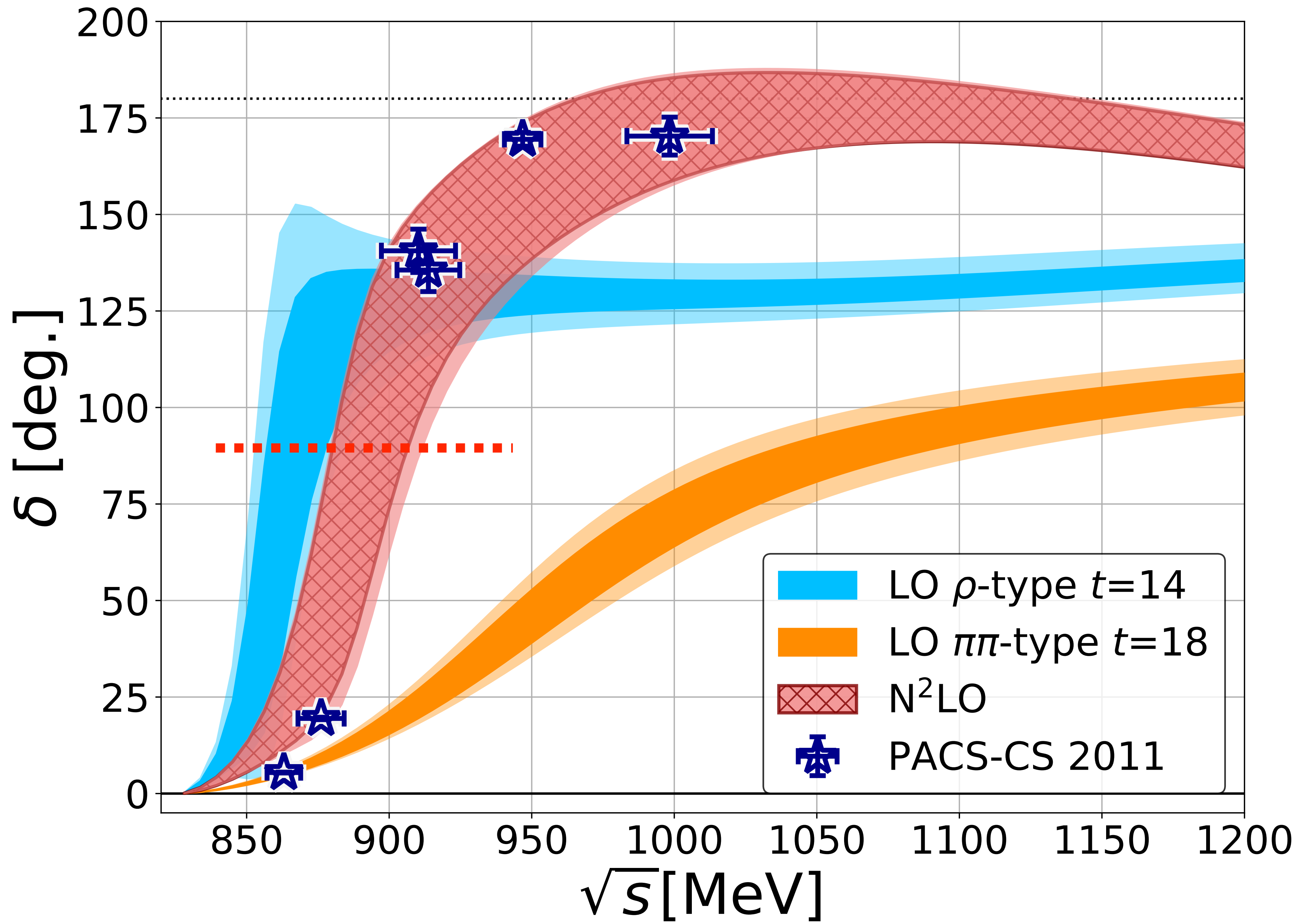

N2LO result almost agrees with the PACS-CS by the FV method.

ρ resonance parameters

Breit-Wigner fit $\dfrac{k^3 \cot \delta_1(k)}{\sqrt{s}} = \dfrac{6\pi}{g_{\rho\pi\pi}^2}(m_\rho^2 - s),$

pole of the S-matrix from N^{2}LO potential

both agree well.

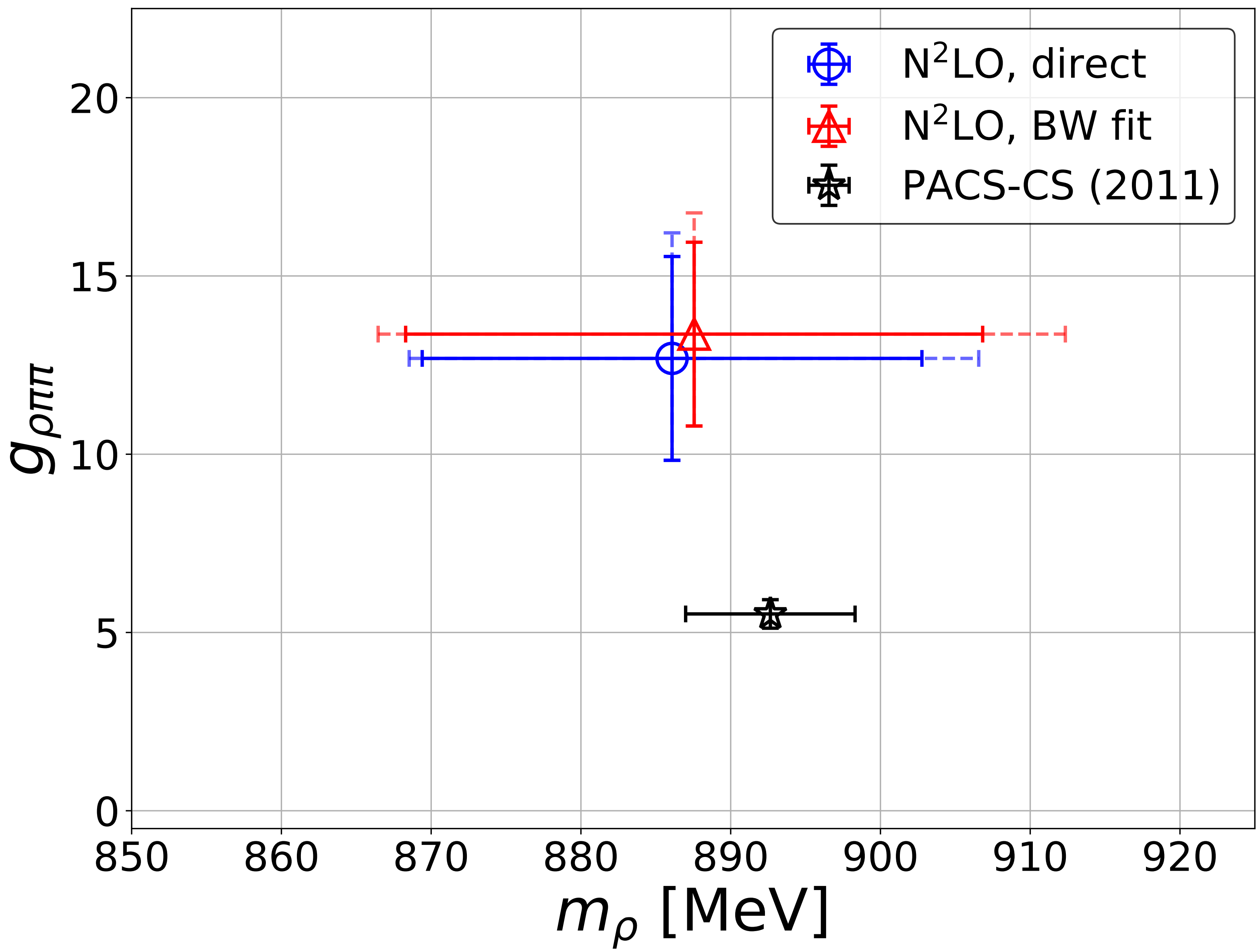

m_ρ from potential agrees with the PACS-CS (FV), while $g_{\rho\pi\pi}$ is much larger.

Probably, the lack of low s states in the center of mass.

IV. HAL QCD potentials in the moving system

Y. Akahori and S. Aoki, in preparation.

σ resonances

σ resonance from $\pi\pi$ scattering in the center of mass system

$$\langle 0|\pi(t)\pi(t)\sigma(0)|0\rangle \simeq \underline{\langle 0|\pi(t)\pi(t)|0\rangle}\langle 0|\sigma(0)|0\rangle + e^{-E_{\pi\pi}t}\langle 0|\pi(t)\pi(t)|\pi\pi\rangle\langle\pi\pi|\sigma(0)|0\rangle$$

vacuum states dominates signals

non-zero total momentum (boosted system)

$$\langle 0|\pi(t)\pi(t)\sigma(0)|0\rangle \simeq e^{-E_{\pi\pi}t}\langle 0|\pi(t)\pi(t)|\pi\pi\rangle\langle\pi\pi|\sigma(0)|0\rangle + \cdots$$

vacuum contribution is absent

HAL QCD method was formulated for a boosted system. S. Aoki, Lattice 2019.

Recently, numerical test for $I = 2$ $\pi\pi$ system has been performed.

IV-1. Theory

S. Aoki, lattice 2019.

Setup

Center of mass (CM)

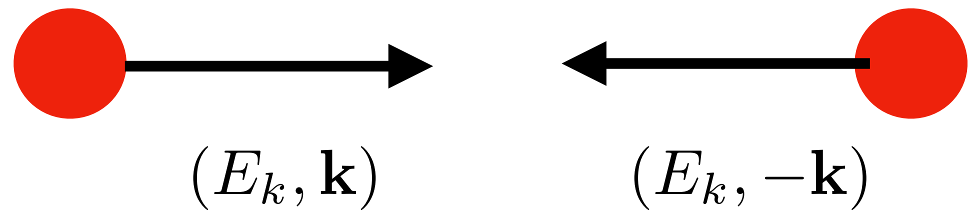

$$\mathbf{P}^* = 0$$

$$E_k = \sqrt{\mathbf{k}^2 + m^2}$$

Moving

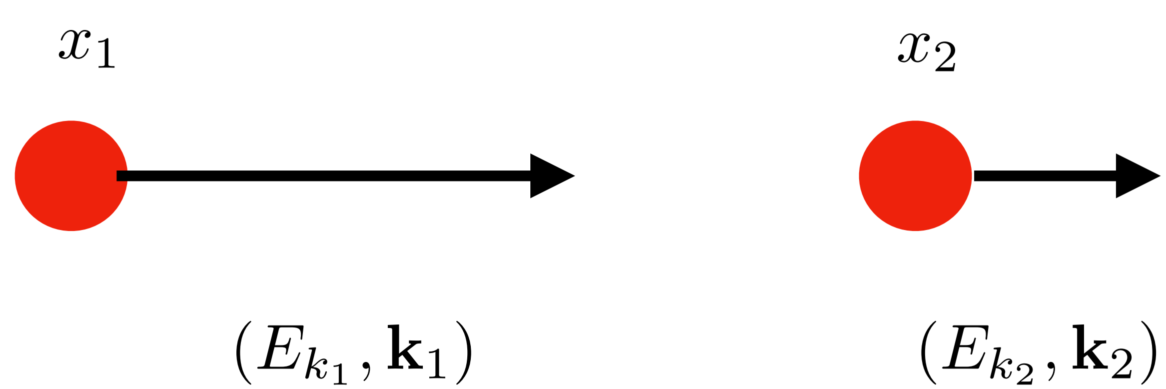

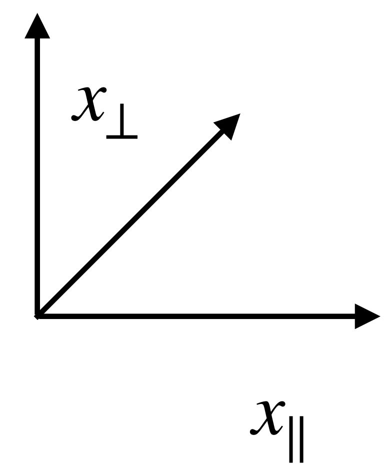

$$\mathbf{P} = \mathbf{k}_1 + \mathbf{k}_2$$

Lorentz transformation

$$\mathbf{P}^* = \gamma(\mathbf{P} - \mathbf{v}W) = 0 \qquad W = \sqrt{\mathbf{k}_1^2 + m^2} + \sqrt{\mathbf{k}_2^2 + m^2} \qquad \gamma := \frac{1}{\sqrt{1 - \mathbf{v}^2}}$$

$$P \cdot X = P^* \cdot X^* \qquad X := \frac{x_1 + x_2}{2}, x := x_1 - x_2$$

HAL QCD potential from boosted NBS wave function

Leading order HAL QCD potential

$$V^{\mathrm{LO}}_{x^{*4}}(\mathbf{x}^*) = \frac{(\nabla^{*2} + k^{*2})\varphi_{k_1^*,k_2^*}(\mathbf{x}^*, x^{*4})}{2\mu\varphi_{k_1^*,k_2^*}(\mathbf{x}^*, x^{*4})}.$$

CM

NBS wave function

$$e^{iP\cdot X}\varphi_{k_1,k_2}(x) = e^{iP^*\cdot X^*}\varphi_{k_1^*,k_2^*}(x^*)$$

Moving CM

$$x^{*4} = \gamma(x^4 - i\mathbf{v}\cdot\mathbf{x}_\parallel), \quad \mathbf{x}^*_\parallel = \gamma(\mathbf{x}_\parallel + i\mathbf{v}x^4), \quad \mathbf{x}^*_\perp = \mathbf{x}_\perp.$$

LO potential $x^4 = \mathbf{x}_\parallel = 0$

Moving

$$V^{\mathrm{LO}}_{x^{*4}=0}(\mathbf{x}^*_\perp) = \left.\frac{(\nabla_\perp^2 + \gamma^2(\nabla_\parallel + i\mathbf{v}\partial_{x^4})^2 + k^{*2})\varphi_{k_1,k_2}(\mathbf{x}, x^4)}{2\mu\varphi_{k_1,k_2}(\mathbf{x}, x^4)}\right|_{x^4=0,\mathbf{x}_\parallel=0}$$

CM Moving

IV-2. Numerical results

$I = 2\ \pi\pi$ potential

Akahoshi and Aoki, in preparation.

Numerical setup

$2+1$ flavor CP-PACS configurations on a $32^3 \times 64$ latttice

Iwasaki gauge action and non-perturbatively improved Wilson quark action

$a \simeq 0.0907$ fm, $m_\pi \simeq 700$ MeV

smeared quark source

case1: $\mathbf{P} = (0, 0, 2\pi/L)$,

case2: $\mathbf{P} = (0, 0, 4\pi/L)$,

CM: $\mathbf{P} = (0, 0, 0)$,

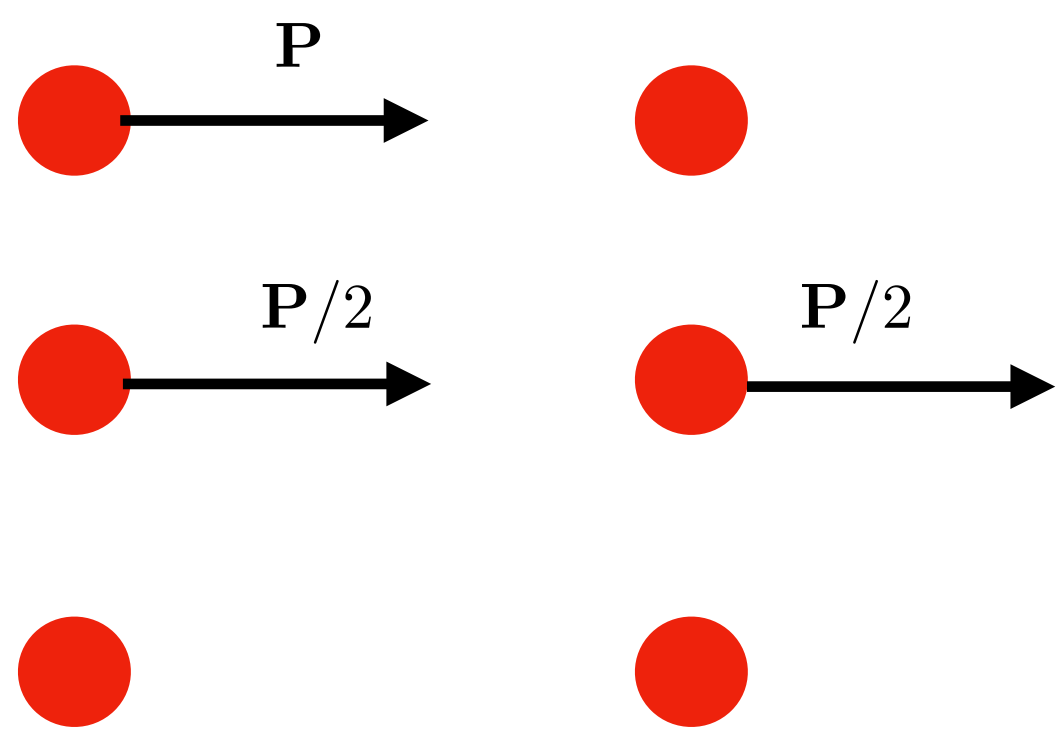

Potentials (breakup)

$$V^{\mathrm{LO}}_{x^{*4}=0}(\mathbf{x}_\perp) = \left.\frac{(L_\perp + L_\parallel)(\mathbf{x}, x^4, X^4)}{mG(\mathbf{x}, x^4, X^4)}\right|_{x^4=0,\mathbf{x}_\parallel=0} + \left.\frac{E(\mathbf{x}, x^4, X^4)}{G(\mathbf{x}, x^4, X^4)}\right|_{x^4=0,\mathbf{x}_\parallel=0}$$

Laplacian

energy

case1

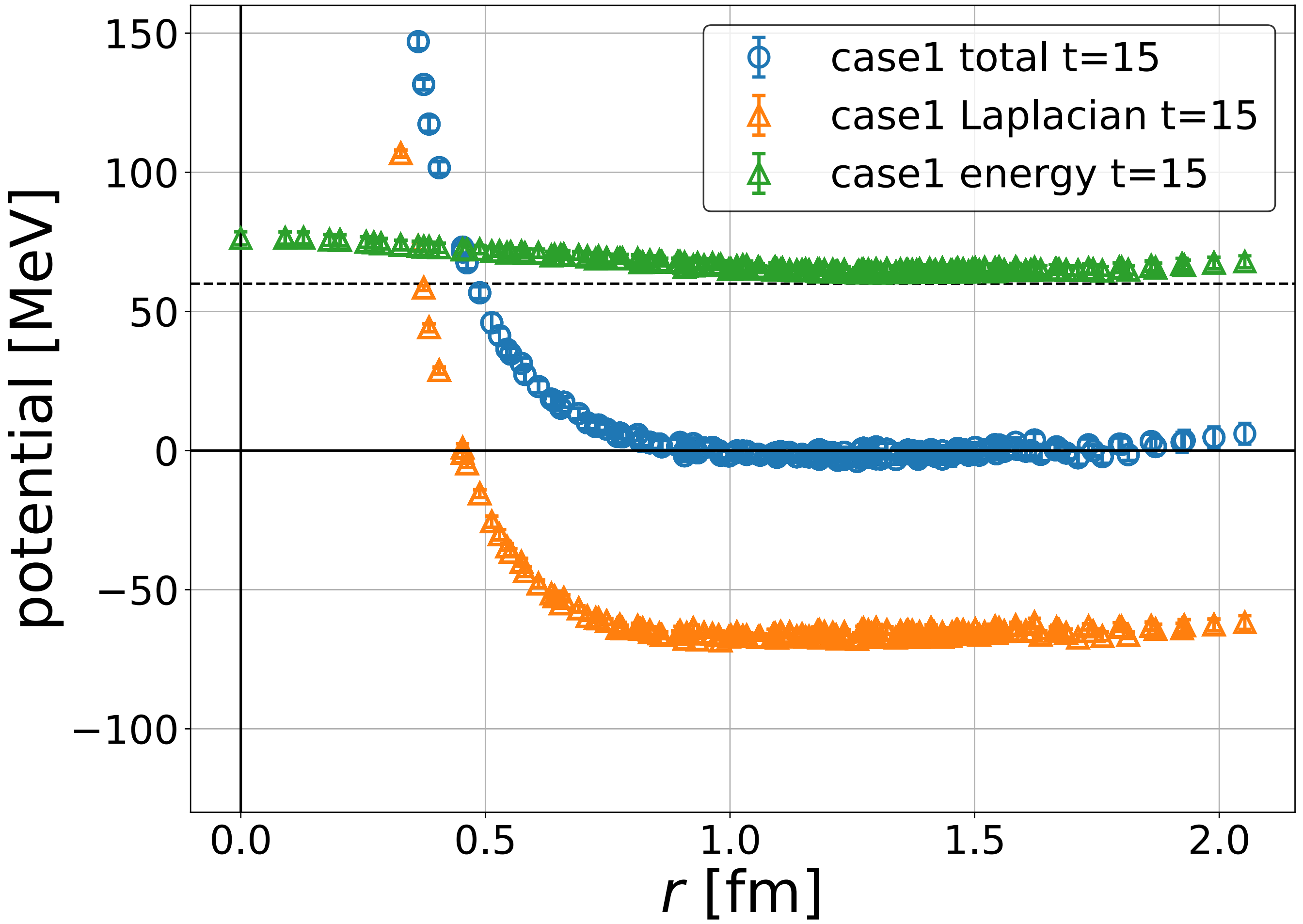

case2

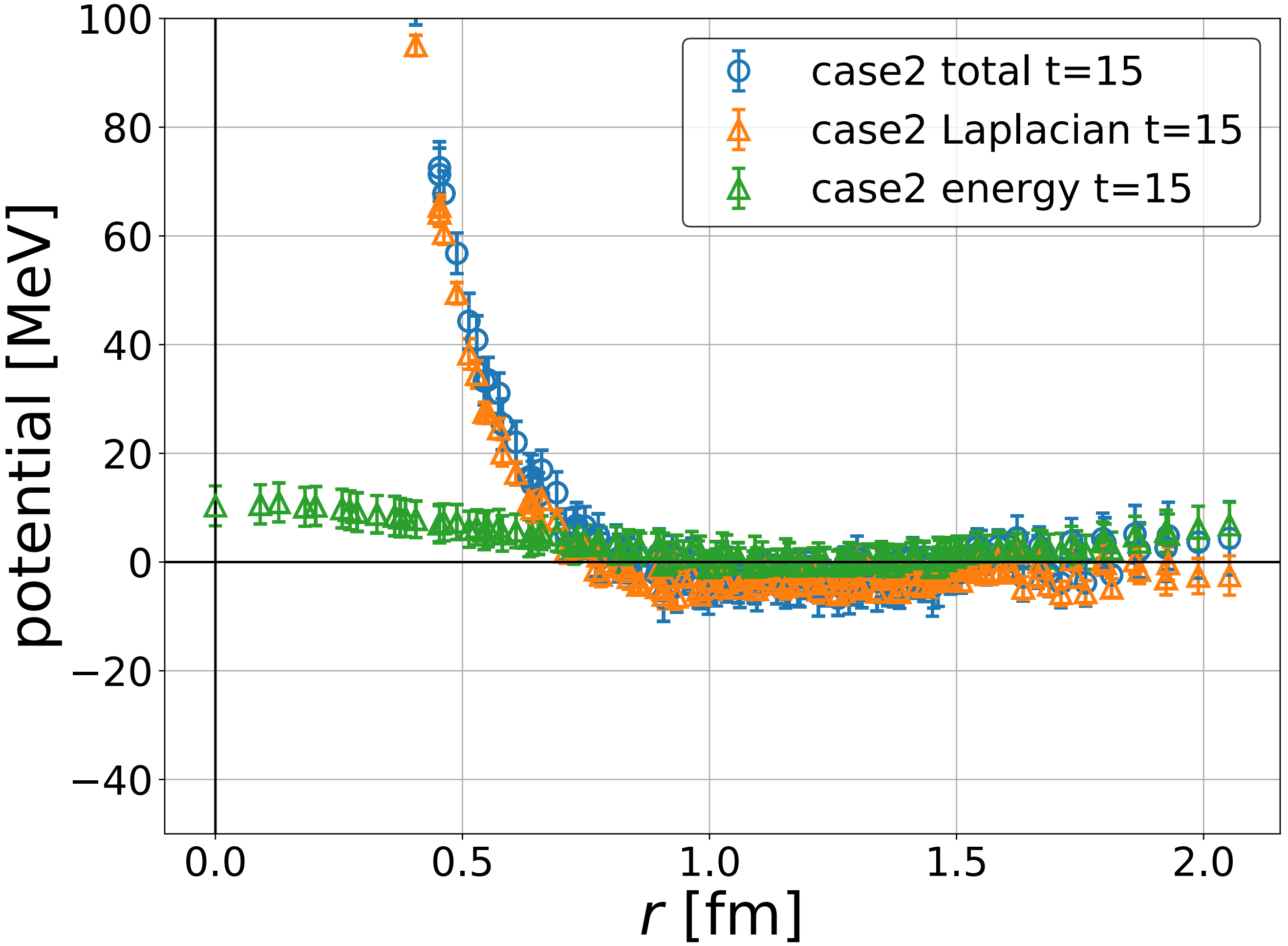

$\simeq$ CM

Potentials (comparison)

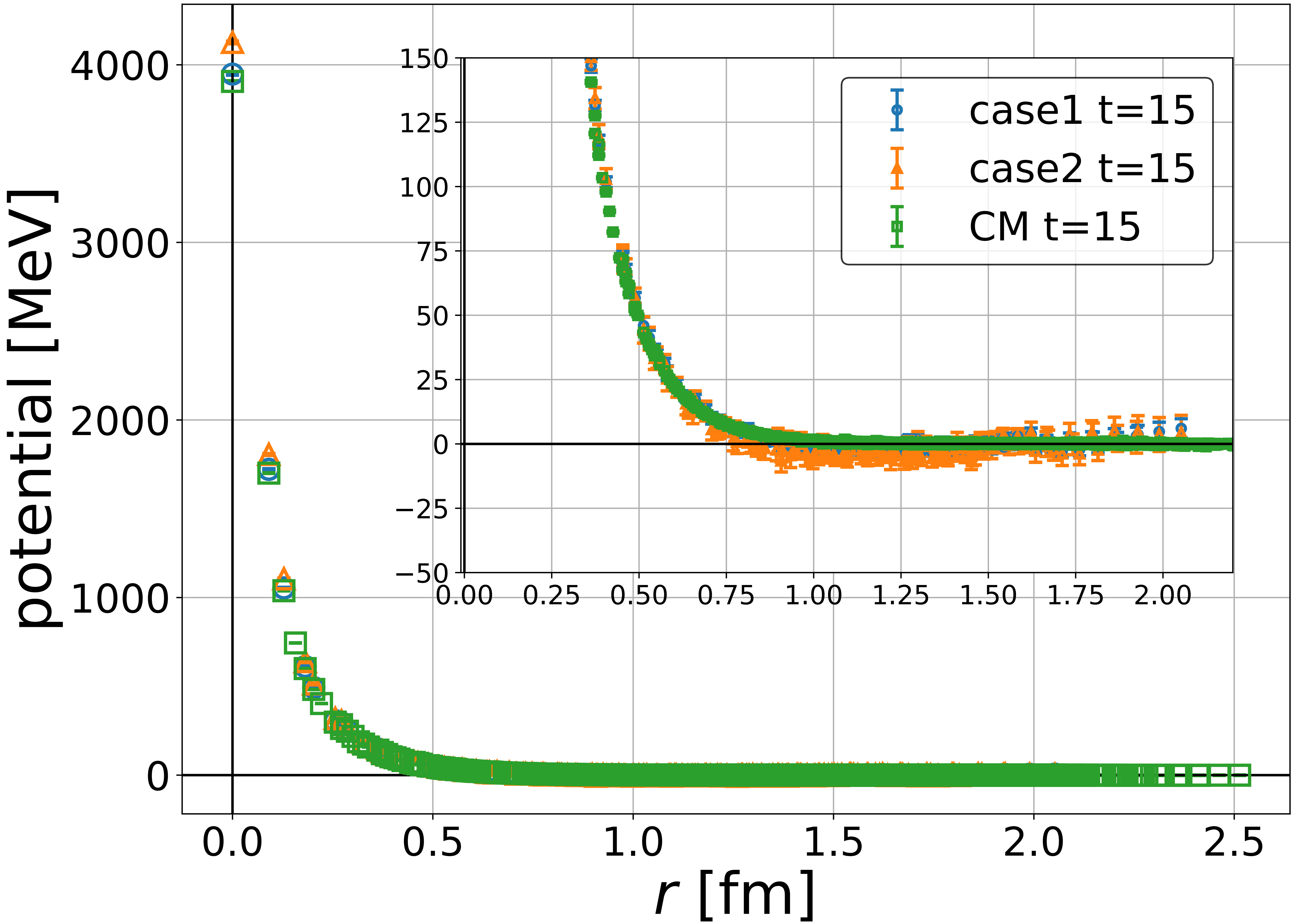

They are consistent except at short distances, though boosted ones are noisier.

Scattering phase shifts

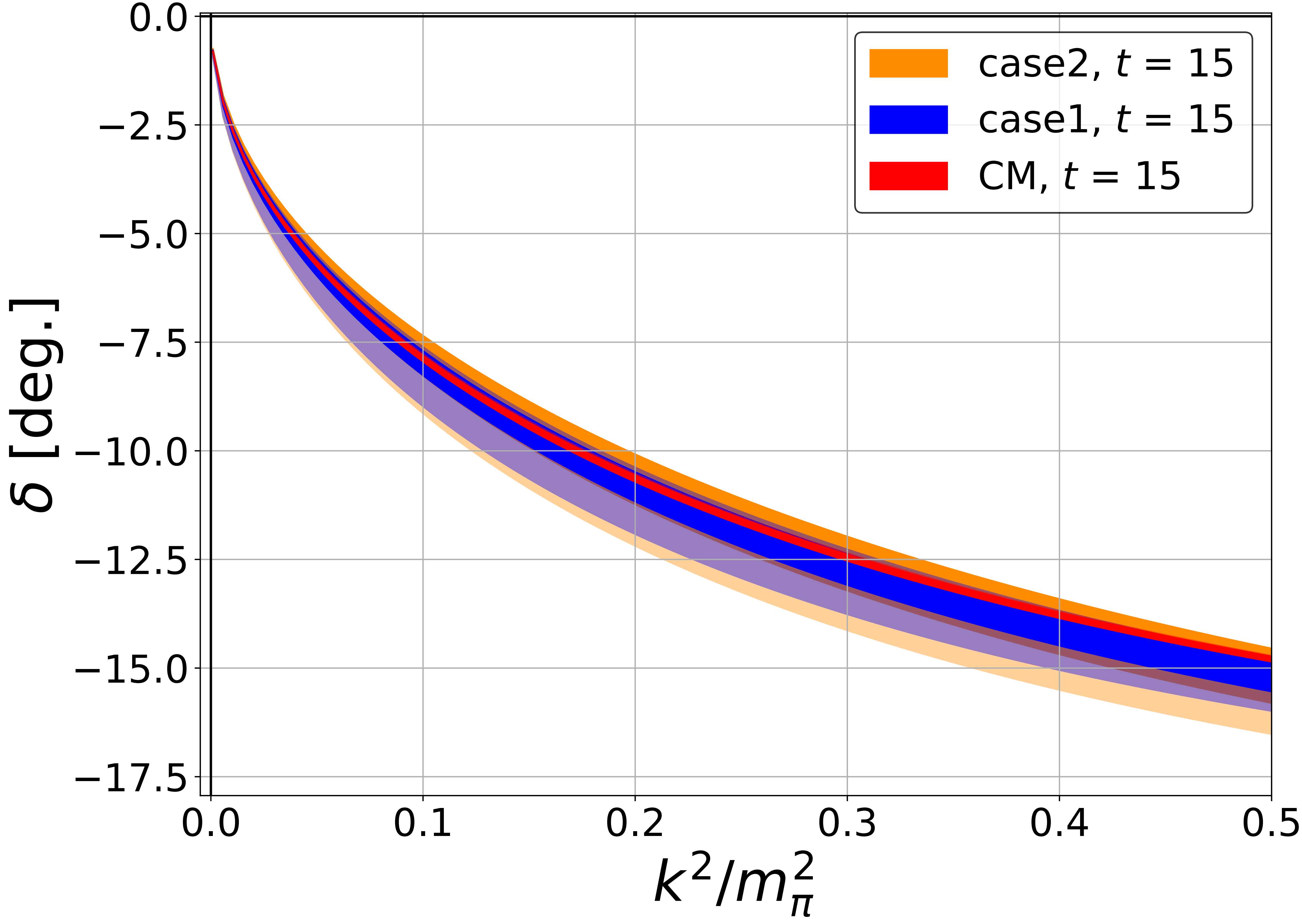

All three cases gives consistent results.

Comparison with finite volume method

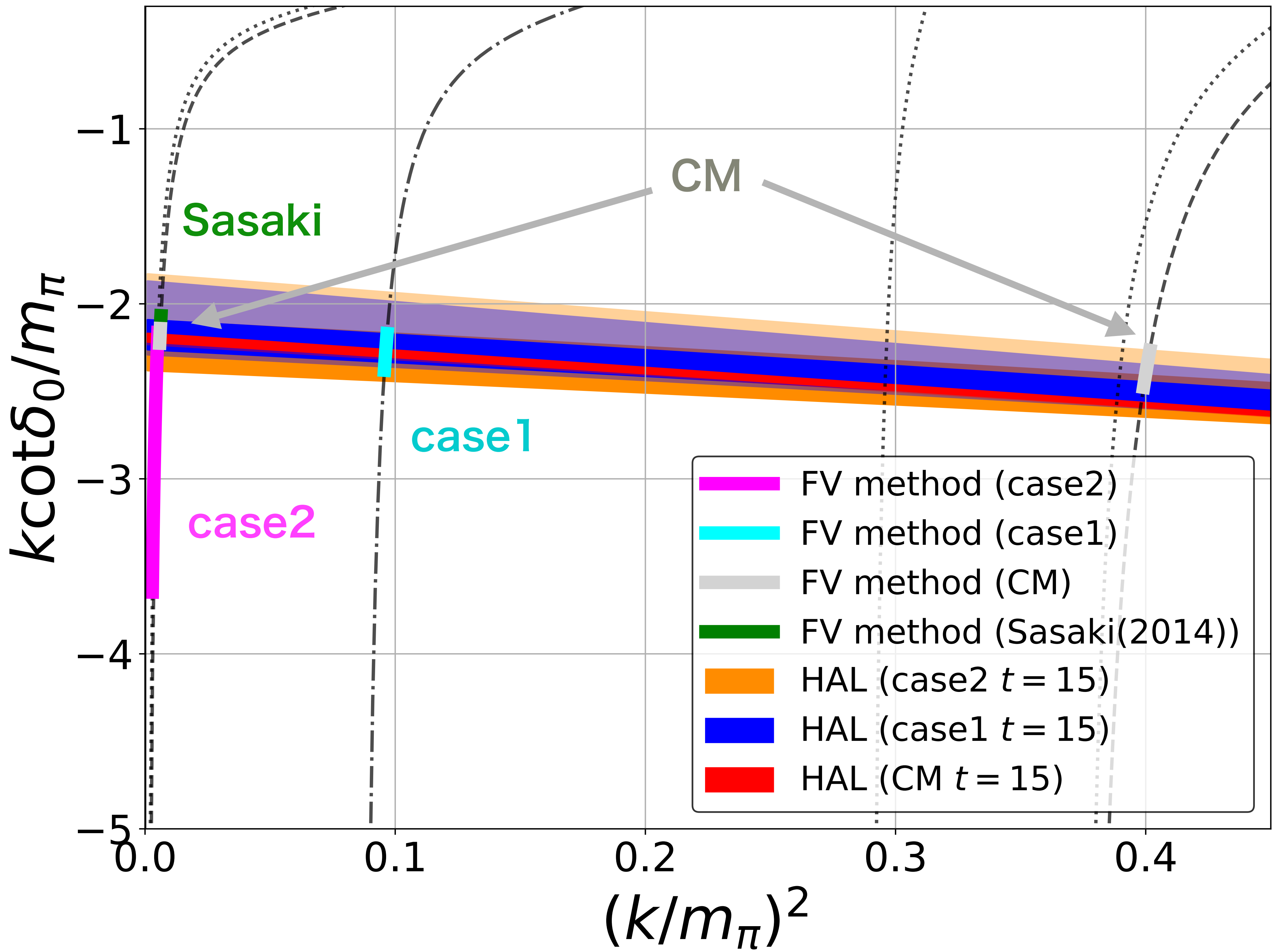

HAL QCD potentials with non-zero momentum work !

Comparison at low energies

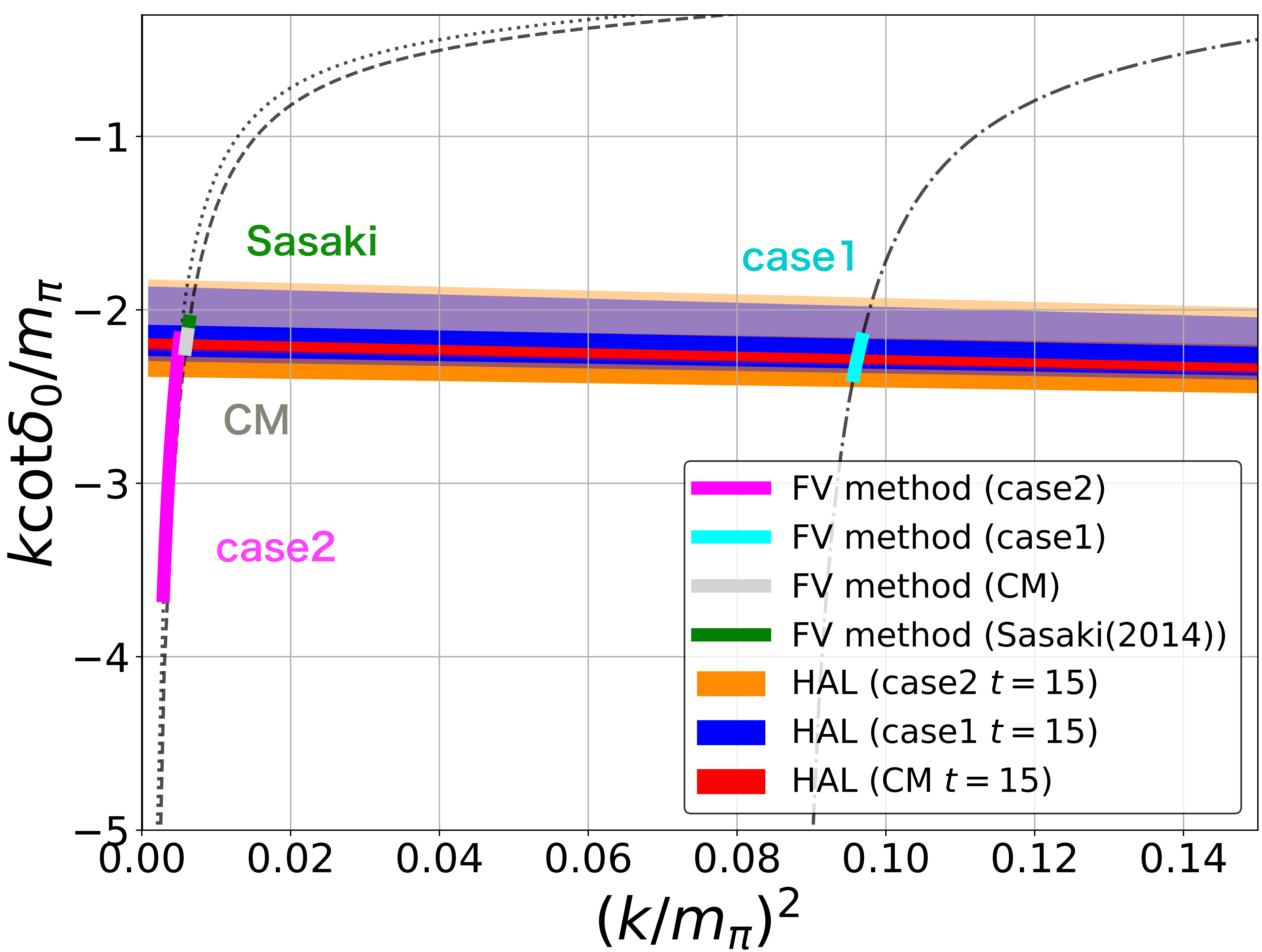

V. Summary and Discussions

- HAL QCD method provides useful tools to investigate not only dibaryons but also hadron resonates such as ρ meson.

- The formula to obtain potential in the HAL QCD method is extended to moving systems, and is shown to work for the $I = 2\pi\pi$ scattering.

HAL QCD method vs. finite volume spectra

A discrepancy that HAL QCD/FV spectra predict unbound/bound NN at $m_\pi \sim 700 - 800$ MeV seems to be resolved recently.

bound NN is disfavored.

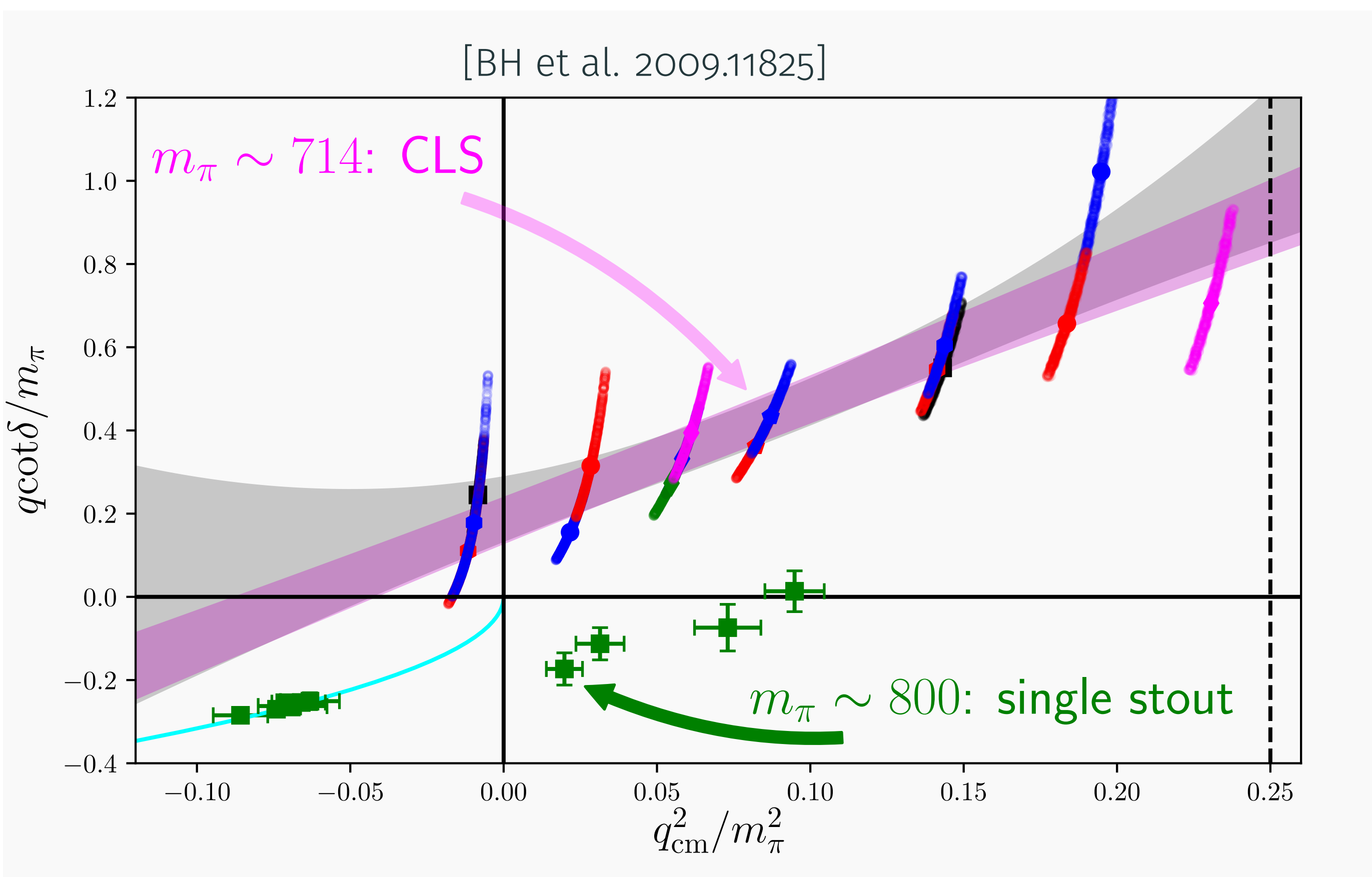

review by B. Hoerz in Lattice2021

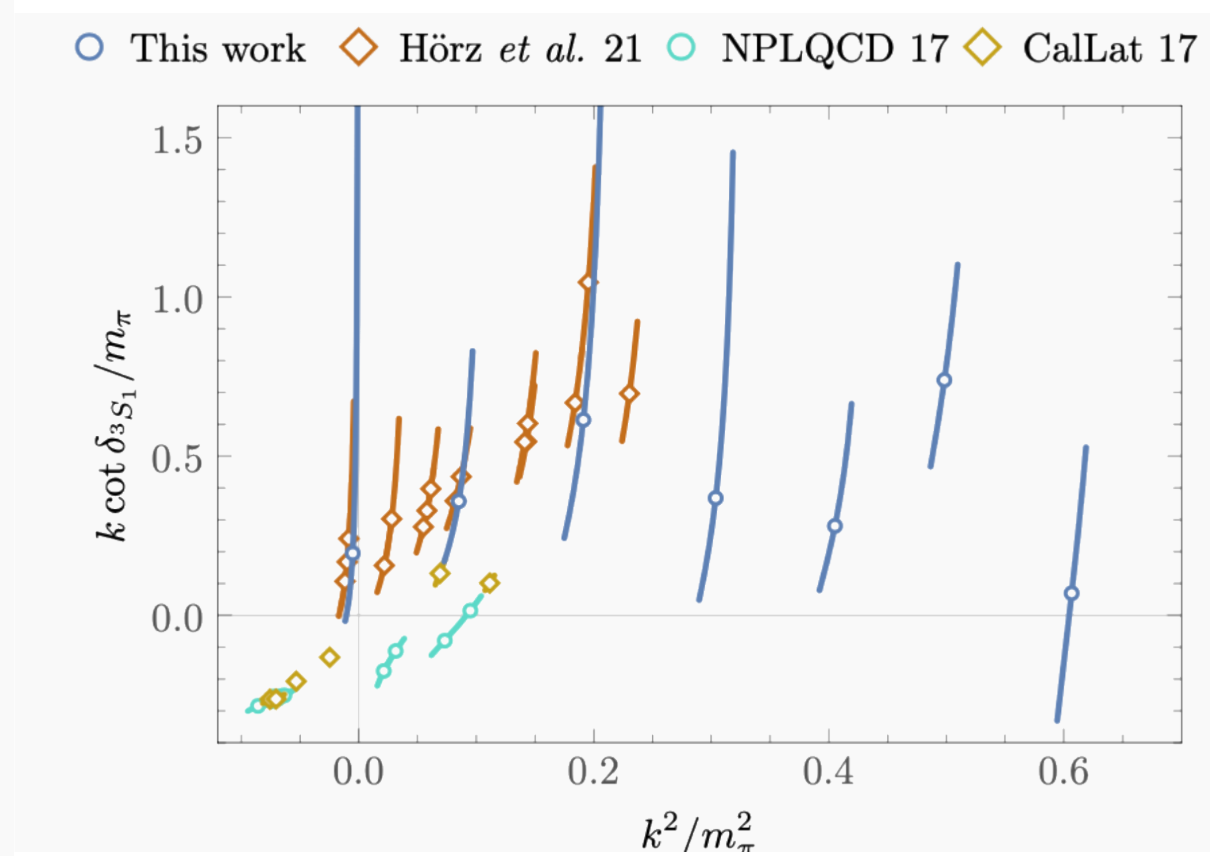

talk by M. Wagman in Lattice2021

Backup

Why $g_{\rho\pi\pi}$ is larger ?

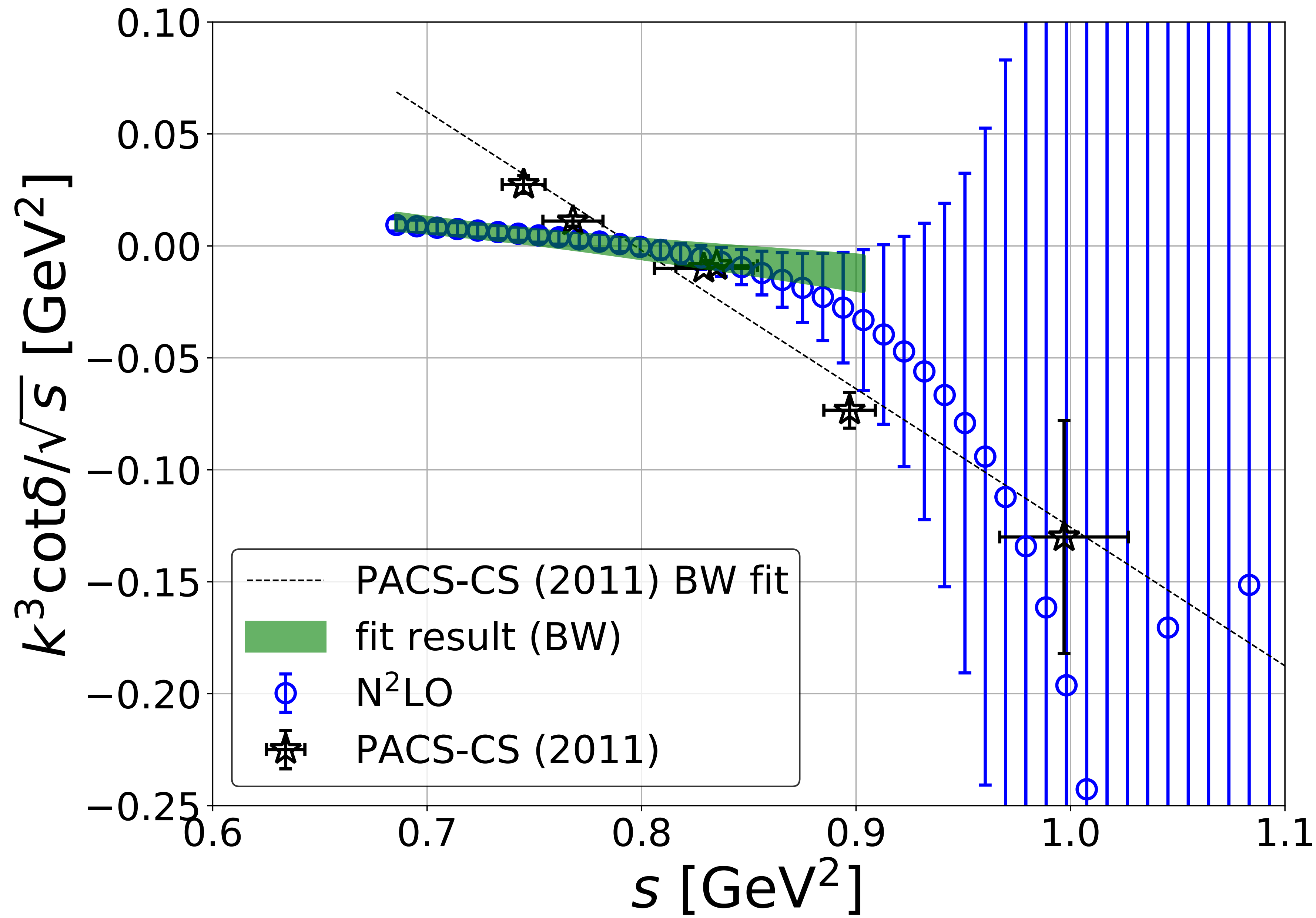

$$\frac{k^3\cot\delta_1(k)}{\sqrt{s}} = \frac{6\pi}{g^2_{\rho\pi\pi}}(m_\rho^2 - s),$$

slope is smaller for the potential result.

Probably, the lack of low s states in the center of mass causes this behavior.

Time dependent method

CM $$\left(-H_0 - \partial_{X^{*4}} + \frac{1}{4m}\partial^2_{X^{*4}}\right) R(\mathbf{x}^*, x^{*4}, X^{*4}) = V^{\mathrm{LO}}_{x^{*4}}(\mathbf{x}^*) R(\mathbf{x}^*, x^{*4}, X^{*4})$$

$$R(\mathbf{x}^*, x^{*4}, X^{*4}) := \sum_n B_n \varphi_{W_n^*}(x^*) e^{-\underline{(W_n^* - 2m)} X^{*4}} + \cdots$$

NBS

Moving $$R(\mathbf{x}, x^4, X^4) \simeq \sum_n B_n \varphi_{W_n}(x) e^{-(W_n - 2m) X^4}$$

$$\boxed{V^{\mathrm{LO}}_{x^{*4}=0}(\mathbf{x}_\perp) = \left.\frac{\left(L_\perp + L_\parallel + mE\right)(\mathbf{x}, x^4, X^4)}{mG(\mathbf{x}, x^4, X^4)}\right|_{x^4=0, \mathbf{x}_\parallel = 0}}$$

$$G(\mathbf{x}, x^4, X^4) = \left((\partial_{X^4} - 2m)^2 - \mathbf{P}^2\right) R(\mathbf{x}, x^4, X^4),$$

$$E(\mathbf{x}, x^4, X^4) = \left[\partial^2_{X^4}/4m - \partial_{X^4} - \mathbf{P}^2/4m\right] G(\mathbf{x}, x^4, X^4),$$

$$L_\perp(\mathbf{x}, x^4, X^4) = \nabla^2_\perp G(\mathbf{x}, x^4, X^4),$$

$$L_\parallel(\mathbf{x}, x^4, X^4) = \left(-(\partial_{X^4} - 2m)\nabla_\parallel + i\mathbf{P}\partial_{x^4}\right)^2 R(\mathbf{x}, x^4, X^4).$$

Finite volume spectra

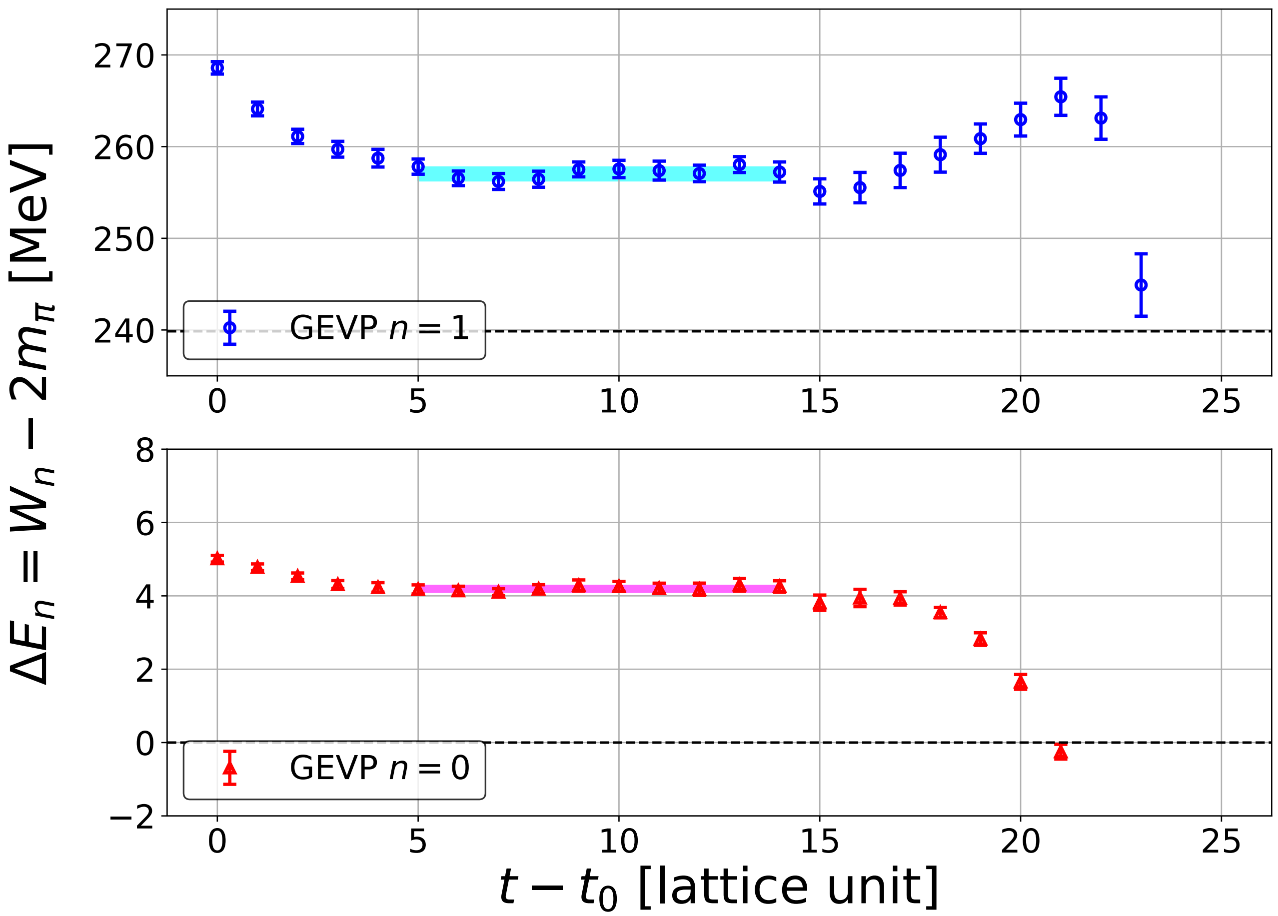

CM (1st excited)

CM (Lowest)

case1 (Lowest)

case 2 (Lowest)